Adaptive PSAM in SIMO Systems with Imperfect CSI in Rayleigh Fading Channels[1]

Reza Barazideh
Department of Electrical Engineering
Shahed University, Tehran, Iran
E-mail: Barazideh@shahed.ac.ir

Babak Seyfe
Department of Electrical Engineering
Shahed University, Tehran, Iran
E-mail: Seyfe@shahed.ac.ir

Abstract

In this paper we provide an adaptive modulation approach that uses adaptive pilot symbols which both pilot spacing and power allocation on pilot symbols are optimized in single input multiple output systems to maximize the spectral efficiency. The maximization is performed in the presence of imperfect channel state information at the transmitter. Also for reduce the computational complexity we propose a new method based on the curve fitting to find optimum power allocation on symbols. We provide closed forms expression for average spectral efficiency and average bit error rate over Rayleigh fading channel. Numerical results show the accuracy of our new method and demonstrate that our adaptive system outperforms other traditional systems that use of non-adaptive pilot symbols with single antenna based on spectral efficiency performance measure.

Keywords: *Adaptive modulation (AM), channel state information (CSI), single input multiple output (SIMO), channel prediction.*

1. Introduction

Adaptive modulation (AM) based on the channel state information (CSI), maximizes the average spectral efficiency (ASE) by adaptation the transmit parameters, such as modulation constellation, transmit power, etc, [1]-[3]. Then the knowledge about the CSI at the transmitter is an essential issue in AM [4]-[8]. According to the transmission delay at the feedback channel and processing delay at both the receiver and the transmitter, the delayed CSI at the transmitter is outdated and is not accurate [5]. So, to fix this problem in adaptive systems, the channel state must be predicted at the receiver and then send back this information to the transmitter [6]. The Channel prediction error effects on the system performance for adaptive coded modulation (ACM) were investigated in [7]. For simplicity in channel prediction, pilot symbols inserted in to data stream, this technique is called pilot symbol assisted modulation (PSAM) [8]-[9]. In traditional techniques, pilot symbols are inserted in to data stream at fixed spacing intervals and allocated powers to those pilot symbols are equal to data symbols power. In [10] both pilot spacing and power allocation between pilot and data symbols are optimized to maximize the ASE. In this paper we use adaptive PSAM for single input multiple output (SIMO) systems by using maximum ratio combining (MRC) at the receiver to maximize the ASE at a targeted bit error rate (BER) via optimization both pilot spacing and power allocation on

---

[1]The material in this paper was presented in part at the 2009 International Conference on Hybrid Information Technology (ICHT) 2009, Daejeon, Korea, August 27 - 29, 2009.

pilot symbols. We also assume that the channel estimation error is negligible compared to the channel prediction error. Because of the large value of the complexity computation of optimum power allocation, we propose a new method based on the curve fitting to find the optimum power allocation on pilot symbols that maximizes the ASE. We propose a function that expresses ASE depends on channel signal to noise ratio (SNR) and power allocation on symbols for different number of receive antennas.

The rest of this paper is organized as follows. Section 2 presents the system model. Section 3 describes the channel prediction and demonstrates effect of channel prediction error on BER performance. Section 4 analyzes the ASE and average BER and outage probability. In section 5 we introduce the new method based on the curve fitting to find optimum power allocation. Numerical results are collected in section 6, and conclusions are drawn in section 7.

The notations we use throughout this paper are as follows. Bold upper (lower) case letters denote matrices (column vectors); $(.)^{-1}, (.)^T, (.)^H$, and $(.)^*$ denote inverse, transpose, Hermitian transpose and conjugate of matrices respectively; $E[.]$ stands for expectation, $\lfloor . \rfloor$ represent the integer floor, and $\mathbf{I}_k$ denotes the $k \times k$ identity matrix.

2. System Model

As depicted in Figure 1, we consider an adaptive system with n_R receive antennas that combines received signals at the receiver with MRC technique. The transmitter adopts its parameters based on the CSI that obtained through feedback channel. The pilot symbols are inserted into data stream after each $L - 1$ data symbols to facilitate the channel prediction, thus the frame structure is according to Figure 2, where D and P denote the data and pilot symbols, respectively. The channel prediction module, predicts the channel at τ second ahead, then based on the predicted channel the pilot spacing and the pilot power and constellation modulation is determined at receiver and then send it back to transmitter through feedback channel. The power sharing module is used to share the power between pilot and data symbols. It is assumed that the channels are independent and identically distributed (i.i.d) with Rayleigh distribution and channels are slowly time varying according to Jakes model with Doppler spread f_d [11]. Let ε_d and ε_{pl} denote the power per data and pilot symbols, respectively, so the received, noisy and faded data and pilot symbols of the μth channel can be written respectively as

$$y_{d,\mu}(k;l) \triangleq \sqrt{\varepsilon_d} h_\mu(k;l) s(k;l) + \eta_\mu(k;l), \tag{1}$$

$$y_{pl,\mu}(k;0) \triangleq \sqrt{\varepsilon_{pl}} h_\mu(k;0) s_{pl}(k;0) + \eta_\mu(k;0), \tag{2}$$
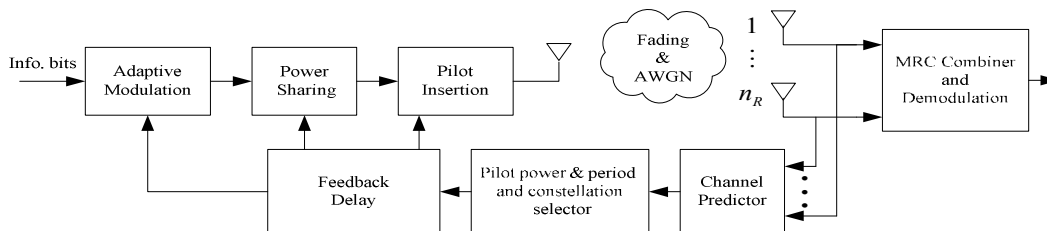

Figure 1. The block diagram of AM system based on adaptive PSAM with receives antennas diversity.
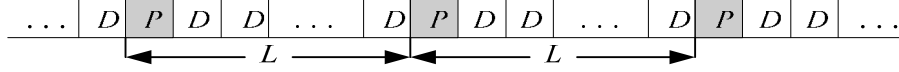
Figure. 2. The transmitted frame structure at the physical layer [10].

where $l \in [1, L-1]$, $\mu \in [1, n_R]$. $\{s(k; l)\}_{l=1}^{L-1}$ are the data symbols, and $\mathrm{s}_{pl}(k; 0)$ is the pilot symbol of the kth frame. We assume that $E(|s(k; l)|^2) = |s_{pl}(k; 0)|^2$ be equal to one; $\eta_\mu(.)$ is the complex additive white Gaussian noise (AWGN) with zero mean and variance $N_0/2$ per dimension; and $h_\mu(k; l)$ denotes the channel coefficient sampled in the lth symbol period of the kth frame, or equivalently at the time $(kL + l)T_s$, where T_s is the symbol period. We also assume that $h_\mu(k; l)$ is a stationary complex Gaussian random process with zero mean and variance $\sigma_h^2 = 1$. Unlike the PSAM in [8], where pilot and data symbols have equal transmit power, in this paper we assume that the pilot and data symbols can be transmitted with different power, similar to [4], [10] and [12], thus as well as the pilot spacing L, the power allocation between pilot and data symbols, must be optimized to maximize ASE while meet the target BER.

3. BER in the presence of channel prediction errors

According to results that are shown in [10] and [14], the estimation error is negligible compared to the prediction error and because MRC is optimum only when the CSI is perfect [13], thus we ignore the channel estimation error. Based on the slow varying channel, we assume that the transmitter adopts its parameters only once per transmission frame of L symbols. Hence the feedback delay is $\tau = JLT_s$, where J is assumed be a positive integer for simplicity. Let $\hat{h}_\mu(k; l)$ be the prediction of $h_\mu(k; l)$, thus the prediction error is $\epsilon_\mu(k; l) = h_\mu(k; l) - \hat{h}_\mu(k; l)$, and the mean square error (MSE) of the predicted channel is $\sigma_{p,\mu}^2(l) = E\left(|\epsilon_\mu(k; l)|^2\right)$. We seek the channel predictor that minimizes the MSE. Define $\mathbf{h}_\mu \triangleq \left[\mathrm{h}_\mu(k-J; 0), \dots, h_\mu(k-J-k_p+1; 0)\right]^{\mathrm{T}}$, the optimal linear minimum mean square error (MMSE) predictor is [7]

$$\mathbf{W}_\mu(l) = \sqrt{\varepsilon_{pl}}\left[\varepsilon_{pl}\mathbf{R}_\mu + N_0\mathbf{I}_{k_p}\right]^{-1}\mathbf{r}_\mu(l), \qquad (3)$$

where $\mathbf{R}_\mu = E\left(\mathbf{h}_\mu\mathbf{h}_\mu^H\right)$ and $\mathbf{r}_\mu(l) = E\left(\mathbf{h}_\mu h_\mu^*(k; l)\right)$ are covariance matrix and covariance vector of $\mathbf{h}_\mu$, respectively. The channel predictor, using k_p past pilot samples $\mathbf{y}_\mu(k; 0) \triangleq \left[y_\mu(k-J; 0), \dots, y_\mu(k-J-k_p+1; 0)\right]^{\mathrm{T}}$, to predict channel coefficients $\{h_\mu(k; l)\}_{l=1}^{L}$, where k_p is the length of the MMSE filter. So the predicted channel is $\hat{h}_\mu(k; l) = \mathbf{W}_\mu^H(l)\mathbf{y}_\mu(k; 0)$ [5], [8] and the MMSE of the predicted channel can be written as [10]

$$\sigma_{p,\mu}^2(l) = 1 - \sqrt{\varepsilon_{pl}}\mathbf{r}_\mu^H(l)\mathbf{W}_\mu(l). \qquad (4)$$

Note that, since the channels assumed to be stationary, the $\sigma_{p,\mu}^2(l)$ does not depend on k. The channels are assumed to be i.i.d, then for each μ we have, $\mathbf{R}_\mu = \mathbf{R}$, $\mathbf{r}_\mu(l) = \mathbf{r}(l)$, and $\mathbf{W}_\mu(l) = \mathbf{W}(l)$, thus the MMSE of all channels are the same and we have $\sigma_{p,\mu}^2(l) = \sigma_p^2(l), \forall\mu$.

Since ε is the average transmit power per symbols, thus $L\varepsilon$ is the total average transmit power for each frame. Because we want to optimize the power allocation, the average power

allocated per data and pilot symbols can be written as $\bar{\varepsilon}_d = \alpha L \varepsilon / (L-1)$ and $\varepsilon_{pl} = (1-\alpha)L\varepsilon$, respectively, where α determines the power allocation between data and pilot symbols and $0 < \alpha < 1$. Let $\mathbf{u}_n$ be the nth eigenvector of $\mathbf{R}$, and λ_n is the corresponding eigenvalue, and $\bar{\gamma}_h$ is the average channel SNR, thus the MMSE of each channel can be expressed as a function of α and L as [10]

$$\sigma_p^2(l) = 1 - \sum_{n=1}^{K_p} \frac{\varepsilon_{pl}|\mathbf{u}_n^H \mathbf{r}(l)|^2}{\varepsilon_{pl}\lambda_n + N_0}$$

$$= 1 - \sum_{n=1}^{k_p} \frac{|\mathbf{u}_n^H \mathbf{r}(l)|^2 (1-\alpha)L\bar{\gamma}_h}{(1-\alpha)L\bar{\gamma}_h \lambda_n + 1}. \tag{5}$$

The total perfect and predicted channels SNR at the receiver after MRC, can be written respectively, as

$$\gamma(k;l) = \frac{\varepsilon_d}{N_0} \sum_{\mu=1}^{n_R} \left| h_\mu(k;l) \right|^2, \tag{6}$$

$$\hat{\gamma}(k;l) = \frac{\bar{\varepsilon}_d}{N_0} \sum_{\mu=1}^{n_R} \left| \hat{h}_\mu(k;l) \right|^2. \tag{7}$$

Let

$$\bar{\gamma} = E[\gamma(k;l)] = \frac{\varepsilon_d}{N_0} \sum_{\mu=1}^{n_R} E\left(\left| h_\mu(k;l) \right|^2 \right)$$

$$= \frac{\varepsilon_d}{N_0} n_R = \varepsilon_1 n_R \bar{\gamma}_h, \tag{8}$$

$$\bar{\hat{\gamma}} = E[\hat{\gamma}(k;l)] = \frac{\bar{\varepsilon}_d}{N_0} \sum_{\mu=1}^{n_R} E\left(\left| \hat{h}_\mu(k;l) \right|^2 \right)$$

$$= \frac{\bar{\varepsilon}_d}{N_0} n_R \left(1 - \sigma_p^2(l) \right) = \varepsilon_2 n_R \bar{\gamma}_h, \tag{9}$$

where $\varepsilon_1 \triangleq \frac{\varepsilon_d}{\varepsilon}$ and $\varepsilon_2 \triangleq \frac{\bar{\varepsilon}_d}{\varepsilon}\left(1 - \sigma_p^2(l)\right)$.

Since the channels are assumed to be Rayleigh, according to (6) and (7), the distribution of perfect and predicted channel SNR after MRC is sum of n_R uncorrelated exponential distribution [15] that can be shown as gamma distribution with shorthand notation $\gamma \sim \mathcal{G}(n_R, \varepsilon_1 \bar{\gamma}_h)$ and $\hat{\gamma} \sim \mathcal{G}(n_R, \varepsilon_2 \bar{\gamma}_h)$ for perfect and predicted channel, respectively [7]. We omitted the time index of $\gamma(k;l)$ and $\hat{\gamma}(k;l)$, for notational brevity. Since γ and $\hat{\gamma}$ are both individually gamma distributed, thus the joint distribution will be a bivariate gamma distribution with shorthand notation $(\gamma, \hat{\gamma}) \sim \mathcal{G}(n_R, \ \varepsilon_1 \bar{\gamma}_h, \varepsilon_2 \bar{\gamma}_h, \rho)$ [7] where ρ is the correlation coefficient of the two variables γ and $\hat{\gamma}$, that can be written as

$$\rho = \frac{cov(\gamma, \hat{\gamma})}{\sqrt{var(\gamma)var(\hat{\gamma})}}$$

$$= \frac{|\mathbf{W}^H(l)\mathbf{r}(l)|^2}{\mathbf{W}^H(l)\mathbf{R}\mathbf{W}(l) + \frac{|\mathbf{W}(l)|^2}{(1-\alpha)L\bar{\gamma}_h}}. \tag{10}$$

We consider a M_n-QAM scheme consisting of N signal constellations with spectral efficiencies $M_n = 2^n$, where $1 \leq n \leq N$. In [1]-[2] it has been shown that the BER of M_n-QAM constellation over an AWGN channel with SNR of γ can be well approximated by

$$BER_n(\gamma) = 0.2 exp\left(-\frac{1.5\gamma}{M_n - 1}\right), \quad n = 1, \dots, N \tag{11}$$

where γ is given by (6). For a chosen constellation M_n, instantaneous BER must be less than the targeted BER and since constellation M_n is chosen based on the predicted channel, thus we need to calculate the $BER_n(\hat{\gamma})$, which can be found as

$$BER_n(\hat{\gamma}) = \int_0^\infty BER_n(\gamma)\, p_{\gamma|\hat{\gamma}}(\gamma|\hat{\gamma})d\gamma, \tag{12}$$

Where $p_{\gamma|\hat{\gamma}}(\gamma|\hat{\gamma})$ is conditional probability density function (PDF) of γ given $\hat{\gamma}$, thus

$$BER_n(\hat{\gamma}) = 0.2 \left(\frac{M_n - 1}{a_n}\right)^{n_R} exp\left(-\hat{\gamma}\frac{1.5\rho\varepsilon_1}{a_n\varepsilon_2}\right), \tag{13}$$

where $\boldsymbol{a_n = 1.5\varepsilon_1\bar{\gamma}_h(1-\rho) + M_n - 1}$. The details of manipulations are shown in the appendix.

4. ASE and average BER and outage probability

4.1. ASE computation

As depicted in Figure 3, the *nth* constellation is chosen when $\hat{\gamma} \in [\hat{\gamma}_n, \hat{\gamma}_{n+1})$, where $\{\hat{\gamma}_n\}_{n=1}^N$ denote the constellation switching thresholds that must be found according to BER constraint, and we define $\hat{\gamma}_0 = 0$ and $\hat{\gamma}_{N+1} = \infty$. In [2] it has been shown that if the symbols chosen from different constellation sizes be transmitted with different power, we have a large computation complexity while the system performance has not significantly improvement. Thus we assume that the transmit power is constant and no data is sent when $\hat{\gamma} < \hat{\gamma}_1$ (Outage is occurred), thus the actual transmit power is [1], [4]

$$\varepsilon_d = \frac{\bar{\varepsilon}_d}{\int_{\hat{\gamma}_1}^\infty p_{\hat{\gamma}}(\hat{\gamma})d\hat{\gamma}} = \frac{\bar{\varepsilon}_d}{Q\left(n_R, \frac{\hat{\gamma}_1}{\varepsilon_2\bar{\gamma}_h}\right)}, \tag{14}$$

where $Q(.,.)$ is the normalized incomplete gamma function [16, eq. 11.3]. Suppose we set the target BER at BER_0, so according to $BER_n(\hat{\gamma}) = BER_0$, the constellation switching thresholds can be written as

$$\hat{\gamma}_n = \frac{a_n\varepsilon_2}{1.5\rho\varepsilon_1} ln\left(\frac{b_n}{BER_0}\right), \quad n = 1, \dots, N \tag{15}$$

Figure 3. SNR range is split into N+1 interval.

where $b_n = 0.2 \left(\frac{M_n - 1}{a_n}\right)^{n_R}$. So the ASE can be expressed as

$$S = \left(1 - \frac{1}{L}\right) \sum_{n=1}^{N} k_n P(k_n)$$

$$= \left(1 - \frac{1}{L}\right) \sum_{n=1}^{N} log_2(M_n) \, P(\hat{\gamma}_n < \hat{\gamma} < \hat{\gamma}_{n+1}), \tag{16}$$

where $k_n \triangleq log_2(M_n)$ and

$$P(\hat{\gamma}_n < \hat{\gamma} < \hat{\gamma}_{n+1}) = \int_{\hat{\gamma}_n}^{\hat{\gamma}_{n+1}} p_{\hat{\gamma}}(\hat{\gamma}) \, d\hat{\gamma}$$

$$= Q\left(n_R, \frac{\hat{\gamma}_n}{\varepsilon_2 \bar{\gamma}_h}\right) - Q\left(n_R, \frac{\hat{\gamma}_{n+1}}{\varepsilon_2 \bar{\gamma}_h}\right), \tag{17}$$

and the maximum value of L is $L_{max} = \left\lfloor \frac{1}{2 f_d T_s} \right\rfloor$, [8].

Since $\sigma_p^2(l)$ depends on α and L, thus the constellation switching thresholds and the ASE depend on α and L. Thus the following optimization problem must be solved

$$\max_{\alpha, L} \; S(\alpha, L). \tag{18}$$

For each $0 < \alpha < 1$ and $L \in [2, L_{max}]$, via numerical search techniques, we can find optimum α and L such that maximize the ASE.

4.2. Average BER computation

The average BER is the ratio the average number of bits in error over the average number of bits transmitted [1], then

$$\overline{BER} = \frac{\sum_{n=1}^{N} k_n \overline{BER}_n}{\sum_{n=1}^{N} k_n P(k_n)}, \tag{19}$$

where $\overline{BER}_n$ is the average BER for nth constellation, that given by

$$\overline{BER}_n = \int_{\hat{\gamma}_n}^{\hat{\gamma}_{n+1}} BER_n(\hat{\gamma}) \, p_{\hat{\gamma}}(\hat{\gamma}) d\hat{\gamma}. \tag{20}$$

By substituting (13) and $p_{\hat{\gamma}}(\hat{\gamma})$ into (20) and aid of results in [7], we obtain

$$\overline{BER}_n = 0.2 \left(\frac{M_n - 1}{d_n}\right)^{n_R} \left(Q\left(n_R, \frac{\hat{\gamma}_n d_n}{\varepsilon_2 \bar{\gamma}_h a_n}\right) - Q\left(n_R, \frac{\hat{\gamma}_{n+1} d_n}{\varepsilon_2 \bar{\gamma}_h a_n}\right)\right), \tag{21}$$

where $d_n = 1.5 \varepsilon_1 \bar{\gamma}_h + M_n - 1$.

4.2. Outage probability computation

Since no data is sent when the received SNR falls below $\hat{\gamma}_1$, the adaptive modulation scheme suffers an outage probability for the first data transmission that given by

$$P_{out} = \int_0^{\hat{\gamma}_1} p_{\hat{\gamma}}(\hat{\gamma})\, d\hat{\gamma} = 1 - Q\left(n_R, \frac{\hat{\gamma}_1}{\varepsilon_2 \bar{\gamma}_h}\right) \qquad (22)$$

As expected, the outage probability depends on the first constellation switching threshold $\hat{\gamma}_1$ and also decreases when the average channel SNR grows.

5. New method to find optimum power allocation α

In this section we proposed a new method based on curve fitting to find optimum α in order to maximize the ASE, which has less computational complexity than the conventional search algorithms. In this method we find a function that express ASE depends on $\bar{\gamma}_h$ and α for different number of receive antennas. Note that according to the optimization problem in previous section, we must optimize the both parameters α and L, but according to the achieved results that are shown in the next section, the optimization of L has small affect on the system performance and optimization of α has more effectiveness on the performance than the optimization of L. So for simplicity and decreasing the computational complexity at the transmitter we assume that L is constant. At this condition the ASE can be written as

$$S_f = -f_1(\bar{\gamma}_h)exp\big(\alpha f_2(\bar{\gamma}_h)\big) + f_3(\bar{\gamma}_h)exp\big(\alpha f_4(\bar{\gamma}_h)\big), \qquad (23)$$

where

$$f_1(\bar{\gamma}_h) = p_{11}\bar{\gamma}_h{}^3 + p_{12}\bar{\gamma}_h{}^2 + p_{13}\bar{\gamma}_h + p_{14}\,, \qquad (24)$$

$$f_2(\bar{\gamma}_h) = \frac{\big(p_{21}\bar{\gamma}_h{}^2 + p_{22}\bar{\gamma}_h + p_{23}\big)}{\big(\bar{\gamma}_h + p_{24}\big)}\,, \qquad (25)$$

$$f_3(\bar{\gamma}_h) = \frac{\big(p_{31}\bar{\gamma}_h{}^2 + p_{32}\bar{\gamma}_h + p_{33}\big)}{\big(\bar{\gamma}_h{}^2 + p_{34}\bar{\gamma}_h + p_{35}\big)}\,, \qquad (26)$$

$$f_4(\bar{\gamma}_h) = \frac{\big(p_{41}\bar{\gamma}_h{}^2 + p_{42}\bar{\gamma}_h + p_{43}\big)}{\big(\bar{\gamma}_h + p_{44}\big)}\,. \qquad (27)$$

Note that the functions $f_1(\bar{\gamma}_h)$ to $f_4(\bar{\gamma}_h)$ for different number of receive antennas have the same form with different parameters that are provided in the table 1.

Table 1. Parameters in (24)-(27) that obtained from curve fitting method for different number of receive antennas.

	p_{11}	p_{12}	p_{13}	p_{14}	p_{21}	p_{22}	p_{23}	p_{24}	p_{31}
$n_R = 1$	0	8.249×10^{-8}	7.756×10^{-5}	3.305×10^{-4}	-1.09×10^{-3}	3.476	658	100.3	6.398
$n_R = 2$	8.853×10^{-13}	-2.107×10^{-10}	3.655×10^{-8}	3.134×10^{-7}	-4.32×10^{-3}	7.952	5000	363.1	7.714
$n_R = 4$	2.764×10^{-13}	7.845×10^{-12}	2.469×10^{-8}	6.793×10^{-8}	-5.97×10^{-3}	10.34	1028	69.75	7.695

	p_{32}	p_{33}	p_{34}	p_{35}	p_{41}	p_{42}	p_{43}	p_{44}
$n_R = 1$	1456	2004	1018	4.521×10^4	-9.505×10^{-5}	0.728	128.7	120.8
$n_R = 2$	1760	1654	716.6	2.474×10^4	-2.266×10^{-4}	0.389	61.35	100.3
$n_R = 4$	632.7	244.2	262	4263	-2.196×10^{-4}	0.1927	55	84.28

So the optimum α can be found by derivation ASE from (23) based on the α, i.e. $\frac{dS_f}{d\alpha} = 0$, then the optimum α is calculated as follows

$$\alpha_{opt} = \frac{ln\left(f_1(\bar{\gamma}_h)f_2(\bar{\gamma}_h)/f_3(\bar{\gamma}_h)f_4(\bar{\gamma}_h)\right)}{f_4(\bar{\gamma}_h) - f_2(\bar{\gamma}_h)}. \tag{28}$$

The accuracy of our proposed method is demonstrated in the next section when the system performance with our proposed curve fitting method is compared with the conventional search method.

6. Numerical results

In this section, we present numerical results for an adaptive system which employs 7 different M_n-QAM constellation corresponding to $M_n = \{2, 4, 8, 16, 32, 64, 128\}$ and we set the number of receive antennas $n_R \in \{1, 2, 4\}$. It is assumed that the carrier frequency is $f_c = 2\ GHz$; and symbol period is $T_s = 5\ \mu s$; and mobile velocity is $v = 108\ km/h$ then the Doppler spread is $f_d = 200\ Hz$. Consider the delay and BER are $\tau = 1\ ms$ and $BER_0 = 10^{-5}$, respectively. We assume that the channel has Jakes' Doppler spectrum and the length of prediction filter is $k_p = 250$. Since $\{\sigma_p^2(l)\}_{l=1}^{L-1}$ will be maximized when $l = L - 1$, thus we take the worse case and calculate $\sigma_p^2(L - 1)$ for each l. So with the small penalty in spectral efficiency [10], the computational complexity reduces with factor L.

Figure 4 shows that the power allocation based on the optimum value of α, affects on the ASE but L does not have a valuable effect on ASE, and then we assume a constant value for L in practice. As shown in Figure 5, the performance of our proposed method based on the curve fitting for different system parameters is near to the performance of conventional search algorithms but with less complexity of computations. The ASE of both proposed methods, i.e. curve fitting, and the search method are shown in Figure 6. As we can see the ASE increases when we have more receive antennas at the receiver. It is shown that when we optimize both the power allocation α and pilot spacing L the ASE is higher than the case where power is equally allocated between pilot and data symbols with fixed L. We can see from Figure 6 that our proposed method based on curve fitting have good accuracy. The ASE slope decreases when channel SNR is high, especially for higher receive antennas. It is because that the maximum constellation size is finite. Figure 7 shows the optimum pilot spacing for different number of receive antennas. As can be seen the distance between two pilot symbols is longer when there are more antennas at the receiver and it increases when SNR grows. Figure 8 shows the optimum power allocation between data and pilot symbols for the proposed method and the search method. As shown in this figure, due to the fact that maximum ratio combining (MRC) maximizes the output SNR, the power allocated to the pilot symbols is lower for more number of the receive antennas, thus the average spectral efficiency increases. The accuracy of our proposed method can be seen in this figure in agreement with the Figure 5 and 6. It is observed

from Figure 9, that the average BER of the both new methods i.e. curve fitting method and search is lower than the targeted BER ($BER_0 = 10^{-5}$), even at the low SNR. Thus our adaptive system meets the BER constraint with a large margin. The outage probabilities for different number of receive antennas and for the proposed and the search method is depicted in Figure 10. The curves in this figure demonstrate that diversity mitigates fading effect such that deep fades are averaged out and the outage is occurred with lower probability.
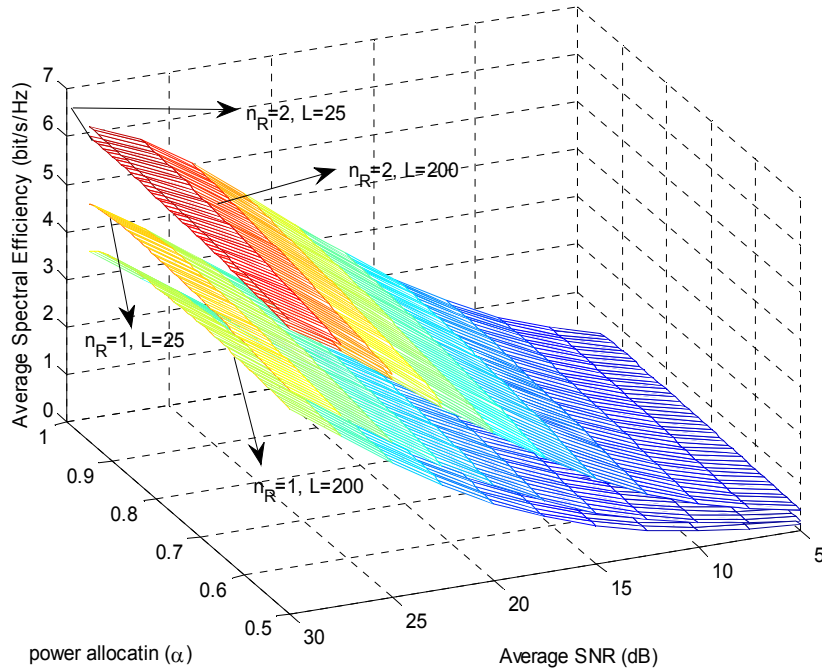
Figure 4. Average spectral efficiency versus average SNR and power allocation α for different pilot spacing $L = \{25, 200\}$. The number of receive antennas is $n_R = \{1, 2\}$, $\tau = 1\ ms$, and $BER_0 = 10^{-5}$.
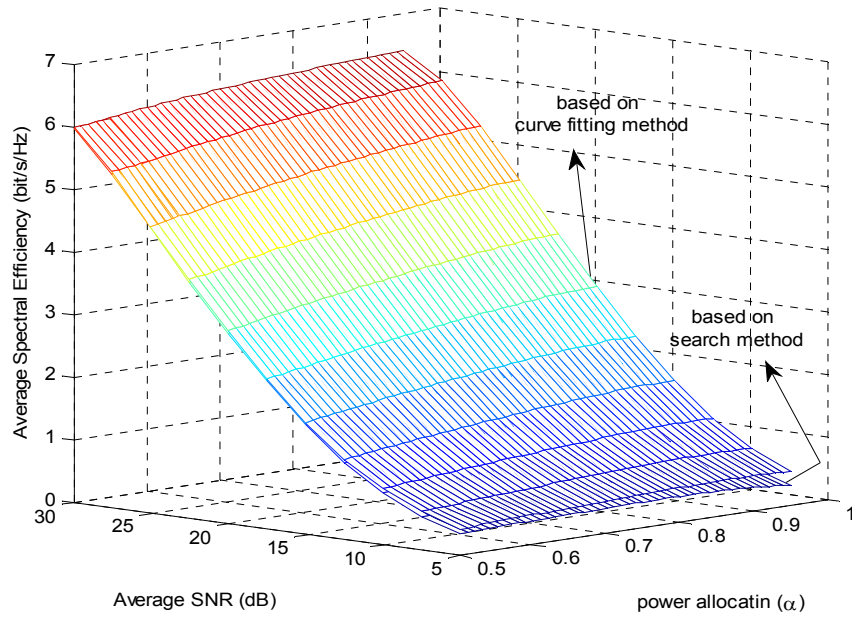
Figure 5. Average spectral efficiency versus average SNR and power allocation α for both search and curve fitting methods and $n_R = 2$, $\tau = 1\ ms$, and $BER_0 = 10^{-5}$.
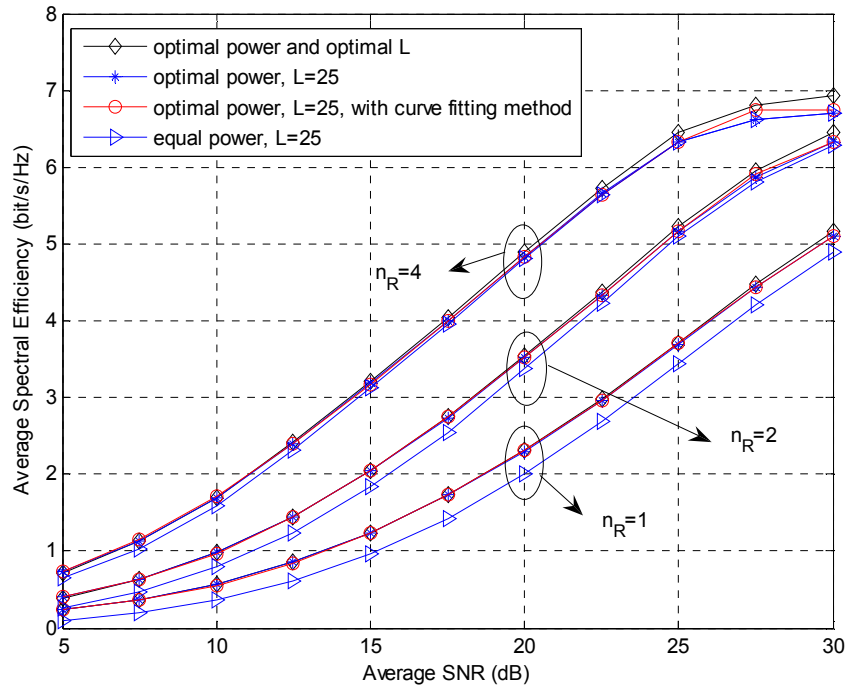

Figure 6. Average spectral efficiency versus average SNR for both optimal parameters and some fixed parameters. The number of receive antennas is $n_R = \{1, 2, 4\}$, $\tau = 1\ ms$, and $BER_0 = 10^{-5}$.
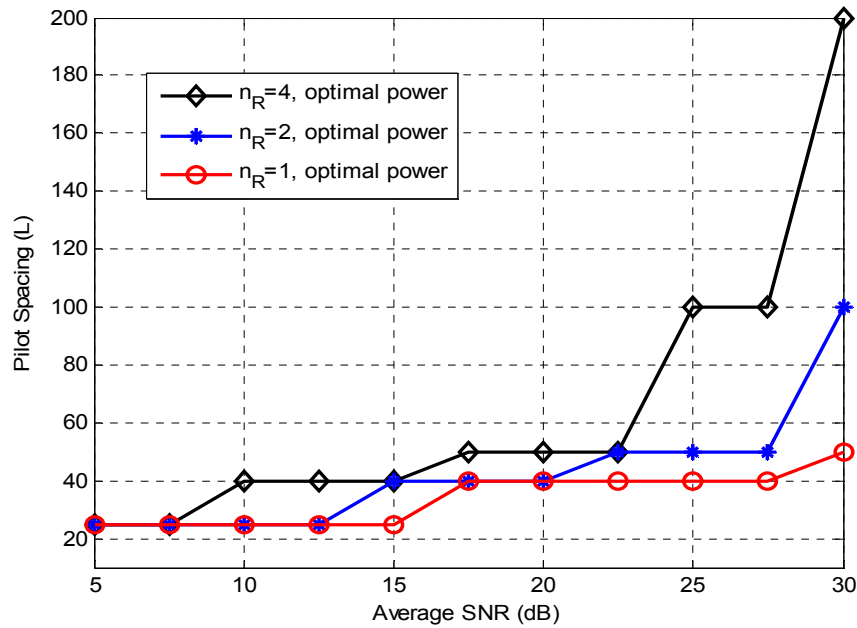
Figure 7. Optimum pilot spacing versus average SNR when power is optimally allocated between the pilot and data symbols. The number of receive antennas is $n_R = \{1, 2, 4\}$, $\tau = 1\ ms$, and $BER_0 = 10^{-5}$.
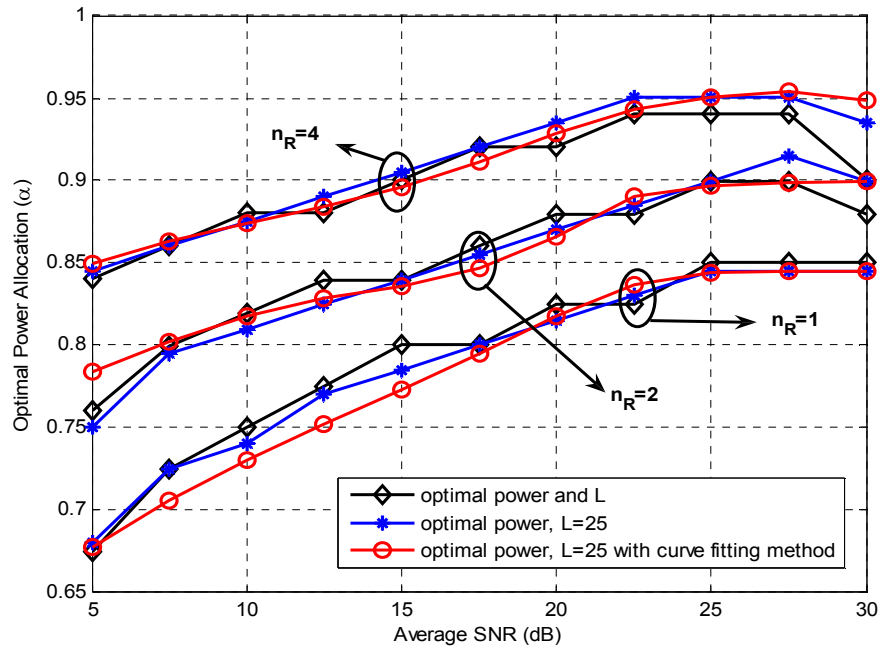

Figure 8. Optimum power allocation to the data symbols versus average SNR when pilot spacing is optimal and $L = 25$. The number of receive antennas is $n_R = \{1, 2, 4\}$, $\tau = 1\ ms$, and $BER_0 = 10^{-5}$.

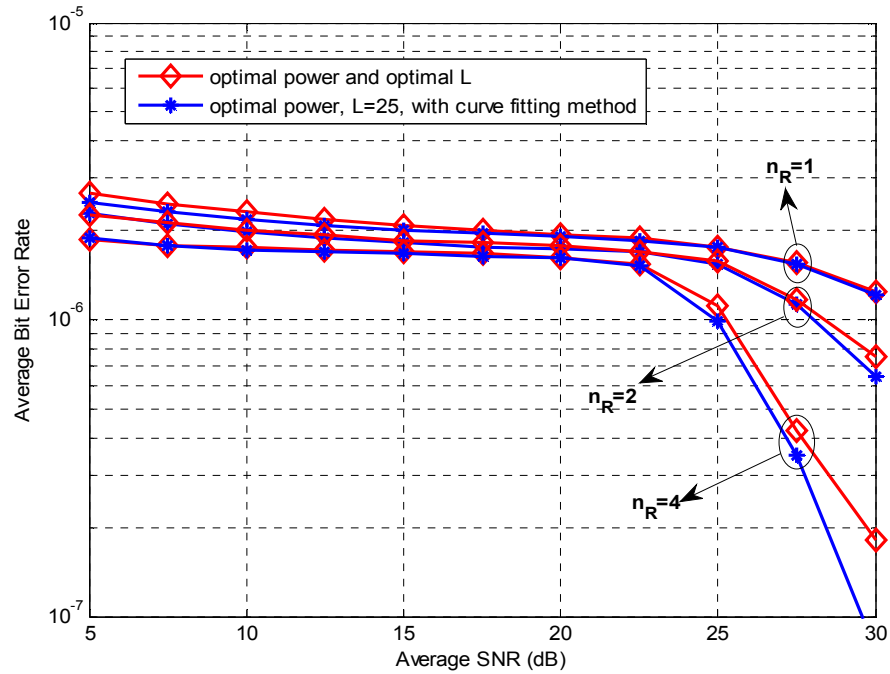**Figure 9. Average bit error rate versus average SNR for optimal power α and optimal pilot spacing L and optimal power with curve fitting method. The number of receive antennas is $n_R = \{1, 2, 4\}$, $\tau = 1\,ms$, and $BER_0 = 10^{-5}$.**

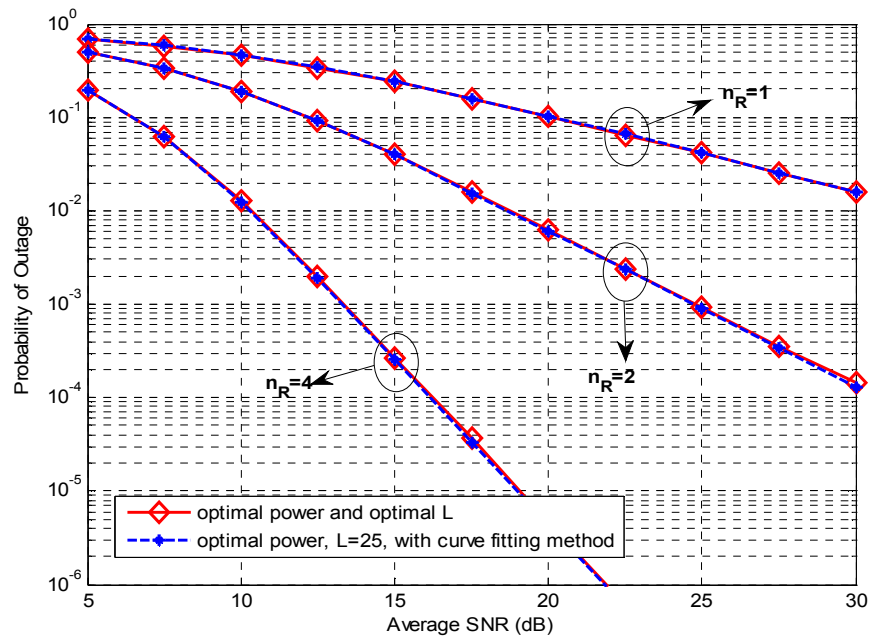**Figure 10. Probability of outage versus average SNR for optimal power α and optimal pilot spacing L and optimal power with curve fitting method. The number of receive antennas is $n_R = \{1, 2, 4\}$, $\tau = 1\,ms$, and $BER_0 = 10^{-5}$.**

7. Conclusion

We have studied an adaptive PSAM with imperfect channel state information where MRC is implemented at the receiver. To maximize the average spectral efficiency, the pilot spacing and power allocation between pilot and data symbols were optimized under prescribed delay and performance constraints. Numerical results show that, when we optimize the power allocation between data and pilot symbols, the optimized pilot spacing does not affect so much on the spectral efficiency. The proposed method based on curve fitting while reduce the computational complexity has very good accuracy. Also we find out that, for more number of receive antennas, the power allocated to the data symbols increases and the outage probability decreases and thus the average spectral efficiency will be increased.

8. Appendix

Derivation of $BER_n(\hat{\gamma})$: At this appendix we calculate the flowing integral

$$BER_n(\hat{\gamma}) = \int_0^\infty BER_n(\gamma)\, p_{\gamma|\hat{\gamma}}(\gamma|\hat{\gamma})d\gamma. \tag{29}$$

According to (11) and [7, eq. 13] and $p_{\gamma|\hat{\gamma}}(\gamma|\hat{\gamma}) = \frac{p_{\gamma,\hat{\gamma}}(\gamma,\hat{\gamma})}{p_{\hat{\gamma}}(\hat{\gamma})}$ we have

$$BER_n(\hat{\gamma}) = \int_0^\infty 0.2\,exp\left(\frac{-1.5\gamma}{M_n-1}\right)\frac{p_{\gamma,\hat{\gamma}}(\gamma,\hat{\gamma})}{p_{\hat{\gamma}}(\hat{\gamma})}d\gamma$$

$$= \frac{0.2}{\bar{\gamma}_h \hat{\gamma}^{\frac{n_R-1}{2}} \varepsilon_1^{\frac{n_R+1}{2}} \varepsilon_2^{\frac{1-n_R}{2}}(1-\rho)\rho^{\frac{n_R-1}{2}}exp\left(\frac{-\hat{\gamma}}{\varepsilon_2\bar{\gamma}_h}\right)} exp\left(\frac{-\hat{\gamma}}{\varepsilon_2(1-\rho)\bar{\gamma}_h}\right)$$

$$\times \int_0^\infty \gamma^{\frac{n_R-1}{2}}exp\left(-\gamma\left(\frac{1.5}{M_n-1}+\frac{1}{\varepsilon_1(1-\rho)\bar{\gamma}_h}\right)\right)I_{n_R-1}\left(\sqrt{\gamma}\frac{2}{(1-\rho)\bar{\gamma}_h}\sqrt{\frac{\rho\hat{\gamma}}{\varepsilon_1\varepsilon_2}}\right)d\gamma, \tag{30}$$

where $I_v(.)$ is the modified Bessel function of the first kind and order v [17, eq. 8.445]. Via using the Nuttall function that defined as [18]

$$\int_y^\infty u^{\frac{H-1}{2}}exp(-u\Phi)I_{H-1}\left(\sqrt{u}2\Psi\right)du = \frac{\Psi^{H-1}}{\Phi^H}exp\left(\frac{\Psi^2}{\Phi}\right)Q_H\left(\frac{\Psi^2}{\Phi},y\Phi\right), \tag{31}$$

where $Q_H(.,.)$ is the generalized Marcum Q-function, that defined as [16]

$$Q_H(x,y) = e^{-x}\sum_{n=0}^\infty \frac{x^n}{n!}Q(H+n,y). \tag{32}$$

Thus with using the correspondences $\Phi = \frac{1.5}{M_n-1}+\frac{1}{\varepsilon_1(1-\rho)\bar{\gamma}_h}$ and $\Psi = \frac{2}{(1-\rho)\bar{\gamma}_h}\sqrt{\frac{\rho\hat{\gamma}}{\varepsilon_1\varepsilon_2}}$ in (31) and some manipulation we get

$$BER_n(\hat{\gamma}) = 0.2 \left(\frac{M_n - 1}{1.5\varepsilon_1 \bar{\gamma}_h (1-\rho) + M_n - 1} \right)^{n_R} exp\left(-\hat{\gamma} \frac{1.5\rho\varepsilon_1}{(1.5\varepsilon_1 \bar{\gamma}_h (1-\rho) + M_n - 1)\varepsilon_2} \right)$$

(33)

9. Acknowledgment

10. References

[1] M. S. Alouini, and A. J. Goldsmith, "Adaptive modulation over Nakagami fading channels", Kluwer J. Wireless Commun., vol. 13, May. 2000, pp. 119–143.

[2] S. T. Chung, and A. J. Goldsmith, "Degrees of freedom in adaptive modulation: A unified view", IEEE Trans. Commun, vol. 49, no. 9, Sep. 2001, pp. 1561–1571.

[3] A. J. Goldsmith, and S.G. Chua, "Variable-rate variable-power MQAM for fading channels", IEEE Trans. Commun, vol. 45, no. 10, Oct. 1997, pp. 1218–1230.

[4] R. Barazideh, and B. Seyfe, "Cross-layer combining of adaptive modulation with truncated ARQ in SIMO systems with imperfect CSI at receiver",IEEE Conf, International conference on communication system, network and application (ICCSNA 2009), vol. 4, Sanya, China, Aug. 2009, pp. 321–325.

[5] S. Zhou, and G. B. Giannakis, "How accurate channel prediction needs to be for adaptive modulation in Rayleigh MIMO channels? ", IEEE Trans. Wireless Commun, vol. 3, no. 4, Jul. 2004, pp. 1285–1294.

[6] A. Duel-Hallen, S. Hu, and H. Hallen, "Long-range prediction of fading signals", IEEE Signal Processing Mag, vol. 17, May. 2000, pp. 62–75.

[7] G. E. Øien, H. Holm, and K. J. Hole, "Impact of channel prediction on adaptive coded modulation performance in Rayleigh fading", IEEE Trans. Veh. Technol, no. 3, May. 2004, pp. 758–769.

[8] J. K. Cavers, "An analysis of pilot symbol assisted modulation for Rayleigh-fading channels", IEEE Trans. Veh. Technol, vol. 40, Nov. 1991, pp. 686–693.

[9] X. Tang, M. S. Alouini, and A. J. Goldsmith, "Effect of channel estimation error on M-QAM BER performance in Rayleigh fading", IEEE Trans. Commun, vol. 47, Dec. 1999, pp. 1856–1864.

[10] X. Cai, and G. B. Giannakis, "Adaptive PSAM accounting for channel estimation and prediction errors", IEEE Trans. Wireless Commun, vol. 4, no. 1, Jun. 2005, pp. 246-256.

[11] W. C. Jakes, Microwave Mobile Communication, Piscataway, NJ: IEEE Press, second edition, 1994.

[12] S. Ohno, and G. B. Giannakis, "Average-rate optimal PSAM transmissions over time-selective fading channels", IEEE Trans. Wireless Commun, vol. 1, no. 10, Oct. 2002, pp. 712–720.

[13] R. You, Li. Hong, and Y. Bar-Ness, "Diversity combining with imperfect channel estimation", IEEE Trans. Commun, vol. 53, no. 10, Oct. 2005, pp. 1655–1662.

[14] G. E. Øien, and K. J. Hole, "Maximum average spectral efficiency for slowly varying Rayleigh fading channels with pilot-symbol-assisted channel estimation", In Proc. European Personal Mobile Communications Conference, Feb. 2001, Vienna.

[15] A. Papoulis, Probability, Random Variables, and Stochastic Processes. New York: McGraw-Hill, 1991.

[16] N. M. Temme, Special Functions: An Introduction to the Classical Functions of Mathematical Physics, John Wiley & Sons Inc, New York, 1996.

[17] I. S. Gradshteyn, and I. M. Ryzhik, Table of Integrals, Series, and Products, Sixth edition, Academic, San Diego, 2000.

[18] A. H. Nuttall, Some integrals involving the Q_M-function. Technical Report 4755. (May 1972), Naval Underwater Systems Center (NUSC), 1972.

Authors

Reza Barazideh received the B.Sc. degree from the Amirkabir University of Technology (Polytechnic), Tehran, Iran, and M.Sc. from Shahed University, Tehran, Iran, both in electrical engineering in 2006 and 2009, respectively. His research interests lie in the areas of communications, signal processing, cooperative network, resource allocation, space-time coding, adaptive modulation, and cross layer design.

Babak Seyfe received the B.Sc. degree from the University of Tehran, Iran, and the M.Sc. and Ph.D. degrees both from Tarbiat Modarres University, Tehran, Iran, all in electrical engineering in 1991, 1995, and 2004, respectively. He was with the Department of Electrical Engineering, Tarbiat Modarres University, Tehran, Iran, in 2004–2005 and a Visiting Researcher with the Department of Electrical and Computer Engineering, University of Toronto, Toronto, ON, Canada, in 2002, and with the Centre for Digital Signal Processing Research, King's College, London, U.K. Currently, he is with the Department of Electrical Engineering, Shahed University, Tehran, Iran. His research interests are detection and estimation theory, statistical signal processing, communication systems, and nonparametric and robust statistics.